JOC The Journal of Organic Chemistry

ARTICLE

pubs.acs.org/joc

Putting the Mechanism of the Soai Reaction to the Test: DFT Study of the Role of Aldehyde and Dialkylzinc Structure

Gianfranco Ercolani* and Luca Schiaffino*

Dipartimento di Scienze e Tecnologie Chimiche, Università di Roma Tor Vergata, Via della Ricerca Scientifica, 00133 Roma, Italy

Supporting Information

ABSTRACT: Previous DFT calculations provided support to the proposal that the Soai reaction involves a mechanism in which dimer catalysts serve as templates for the reaction of two molecules of dialkylzinc with two molecules of aldehyde so as to reproduce themselves (ref 11). Here it is shown that, from the point of view of formal kinetics, this mechanism can be reduced to a general model, dubbed the extended dimer model, that has the Blackmond−Brown dimer model as a particular case. Depending on the interplay of kinetic constants, the extended dimer model can give rise to either chiral amplification or depletion. Calculations of the kinetic constants at the M05-2X/6-31G(d) level of theory were carried out in order to theoretically evaluate the effect of the second aza group in the six-membered aromatic ring of the aldehydic substrate and the effect of dialkylzinc structure. Predictions of chiral amplification or depletion are in striking agreement with experimental data thus lending support to the proposed mechanism.

INTRODUCTION

The Soai reaction, i.e. the autocatalytic asymmetric addition of diisopropylzinc to pyrimidinyl aldehydes, is a unique reaction showing a spectacular chiral amplification (Scheme 1).[1]

The reaction may be selectively triggered solely by the tiny enantiomeric excess (ee) provided by optically active solvent impurities,[2] by statistical fluctuations in the enantiomeric composition of cryptochiral racemic mixtures,[3] by added chiral inducers (e.g., quartz),[4] and even by $^{12}C/^{13}C$ carbon isotope chirality.[5] Since these characteristics might be in common with reactions responsible for the origin of homochirality in nature, there is a growing interest in the mechanism of the Soai reaction.[6,7] To date one of the most prominent mechanisms is the Blackmond−Brown (BB) dimer model supported by kinetics and NMR spectroscopy.[7−10] The principal findings supporting the BB mechanism are the following: (i) homochiral dimers of **2**, in contrast to the heterodimer, are catalytically active,[7a] (ii) homo- and heterochiral dimers are in statistical equilibrium with each other at ambient temperature and significantly associate with iPr$_2$Zn,[7c,f] and (iii) the reaction rate is first order in the homochiral dimers, second order in aldehyde, and zeroth order in iPr$_2$Zn.[7b] To translate the BB mechanism at the molecular level, we made the working assumption that all the association processes occurring in solution are fast and reversible whereas the transfer of the isopropyl group from zinc to aldehyde is irreversible and rate limiting.[11] The consequence of this assumption, given the observed kinetic orders, is that the rate limiting transition state must contain two molecules of alkoxide **2**, two molecules of aldehyde **1**, and an undetermined number of iPr$_2$Zn molecules. In other words, this assumption implies that the molecularity of the reaction, apart from an undetermined number of iPr$_2$Zn molecules in the rate-determining transition state, coincides with the reaction order. With the help of DFT calculations we succeeded in modeling a putative transition state with two molecules of iPr$_2$Zn, which in turn allowed us to propose the autocatalytic cycle illustrated in Scheme 2.[11]

Scheme 1. The Soai Autocatalytic Reaction with 2-Methylpyrimidine-5-carbaldehyde[a]

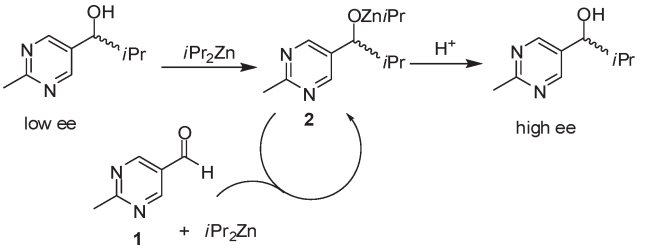

[a] The methyl group in the 2-position of the pyrimidine ring may be replaced with other groups.

The cycle begins with the dimer of **2**-*R*, **3**-R_2, which binds two molecules of iPr$_2$Zn to yield the adduct **4**-R_2. The latter undergoes isomerization to the active form of the catalyst **5**-R_2, which upon binding two molecules of aldehyde **1** yields **6**-*R*,*anti*-*R*,*anti*-*P*. The hexamolecular complex **6**-*R*,*anti*-*R*,*anti*-*P* evolves toward the rate-determining transition state, in which one of the two symmetrically equivalent Zn-bound isopropyl groups, for example, that encircled in the **6**-*R*,*anti*-*R*,*anti*-*P* structure, irreversibly attacks the aldehydic carbon next to it, marked by a large black

Received: December 20, 2010
Published: March 14, 2011

Scheme 2. Homocatalytic Cycle of the Homochiral Dimer 3-R_2

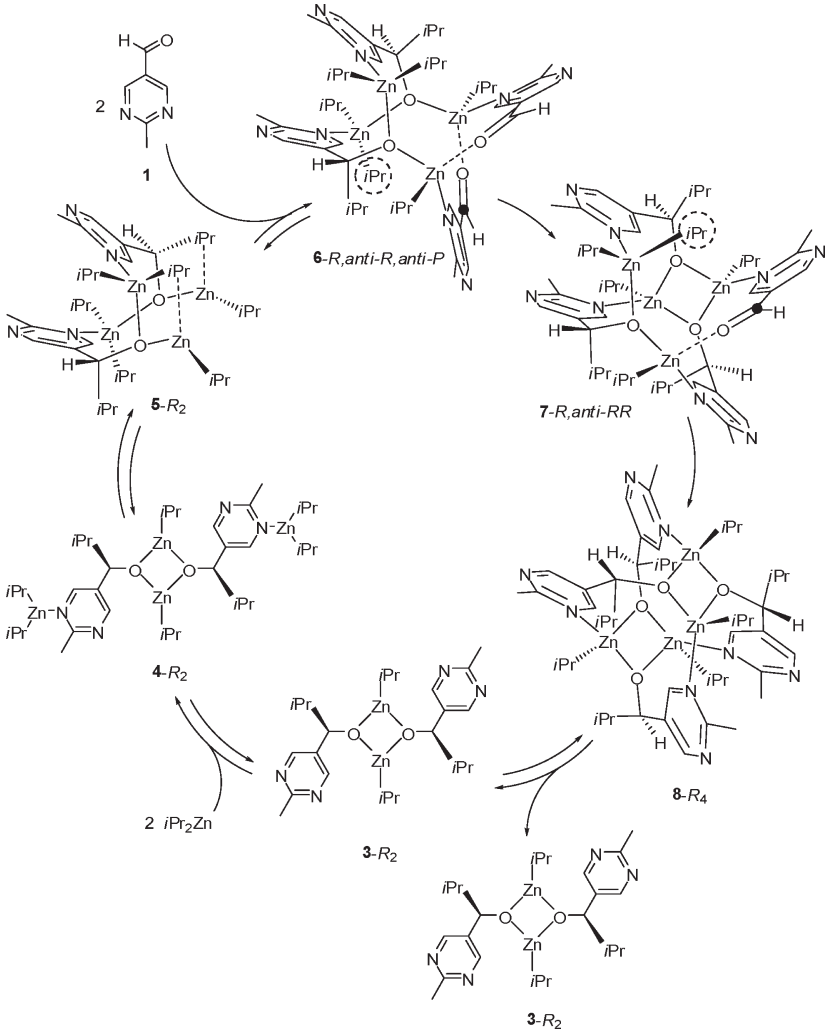

dot, to yield, after interaction of the ex-aldehydic oxygen atom with the nearby zinc center, the pentamolecular complex **7**-*R*,*anti-RR*. Fast and irreversible attack of the Zn-bound isopropyl group encircled in the **7**-*R*,*anti-RR* structure to the remaining aldehyde transforms the complex **7**-*R*,*anti-RR* into the tetramer **8**-R_4. Finally, the tetramer **8**-R_4 dissociates to yield two dimers **3**-R_2, each of which begins a new catalytic cycle. In the complex **6**-*R*,*anti-R*,*anti-P*, each of the isopropyl groups being transferred is correctly oriented to attack the *Re* face of the aldehyde, so that the addition product reproduces the chirality of the *R* catalyst acting as template. Of course the autocatalytic cycle of the homochiral dimer **3**-S_2 (the mirror image of Scheme 2) is also operating. The two enantiomeric cycles are chemically connected through statistical equilibration of the two homodimers and the heterodimer (e.g., **3**-R_2 + **3**-S_2 ⟺ 2 **3**-*RS*). Chiral amplification is warranted by the fact that the heterochiral dimer **3**-*RS* is ineffective as catalyst, and the observed rate independence of the concentration of *i*Pr_2Zn indicates that the resting state at 25 °C is constituted by zinc-saturated dimers.

We remark that the hexamolecular complex **6**-*R*,*anti-R*,*anti-P* is a hypothetical intermediate that has not been experimentally detected, and that its rate-determining conversion to **7**-*R*,*anti-RR* is a consequence of the assumption that all the association processes are fast and reversible. Of course other mechanisms can be, and actually have been,[6g,i] formulated in which, as a consequence of the presence of a complex chemical net involving multiequilibrated intermediates, the kinetic orders do not coincide with molecularity. One should not forget, however, that a reaction mechanism is a hypothesis that may never be said to be proved, but that becomes established through the accumulation of experimental evidence consistent with it.[12] All the proposed mechanisms stand on an equal footing, until some new experimental fact reveals an inconsistency requiring rejection or modification of one or more of them.

To put the mechanism here proposed to the test we wanted to investigate whether it could account for two puzzling aspects of the Soai reaction that up to now have not found any adequate explanation. One is related to the structure of the aldehyde:[13] the addition of *i*Pr_2Zn to pyridine-3-carbaldehyde, **9**, in the presence of a catalytic amount of the reaction product (20 mol %, ee 86%) yielded a product with a final ee of 47% (the ee of the newly formed product is 35%);[14] this result contrasts with the addition of *i*Pr_2Zn to pyrimidine-5-carbaldehyde, **10**, in the presence of a catalytic amount of the reaction product (20 mol %, ee 39%), yielding a product with a final ee of 76% (the ee of the newly formed product is 87%).[1a]

dx.doi.org/10.1021/jo102525t |*J. Org. Chem.* 2011, 76, 2619–2626

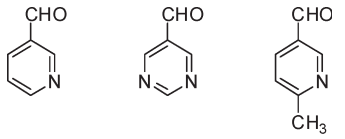

9 10 11

It appears that the presence of one aza group in the six-membered aromatic ring as in **9** leads to depletion of chirality, whereas the presence of a second properly placed aza group as in **10** leads to amplification of chirality. Upon inspection of the mechanism in Scheme 2, the necessity of an aza group for the self-assembly of the transition state is evident, but it is unclear why the chiral amplification is favored by the presence of a second aza group in the 3-position. A second question is related to the structure of the dialkylzinc: Soai's group tested the behavior of Me_2Zn, Et_2Zn, Pr_2Zn, iPr_2Zn, and Bu_2Zn in the reaction with **9**.[14,15] Although with this substrate all the used dialkylzinc showed depletion of chirality, iPr_2Zn did so to a lesser extent, accordingly it became the organozinc reagent of choice for all the successive studies of the Soai group. Brown and Gridnev found that dicyclopropylzinc, tBu_2Zn, and dicyclopentylzinc, in contrast with iPr_2Zn, are not suitable to obtain asymmetric autocatalysis in the reaction with 2-trimethylsilylethynylpyrimidine-5-carbaldehyde.[9a] Thus it appears that iPr_2Zn plays a crucial role for the effectiveness of the Soai reaction. A consistent mechanism should explain why.

Here we report a DFT computational study at the M05-2X/6-31G(d) level of theory aimed at verifying whether the proposed mechanism for the Soai reaction is capable of accounting for such puzzling results. The structure of this paper is as follows. In the first subsection of the Results and Discussion, the formal kinetics of the extended dimer model is presented. In the second subsection, results of DFT calculations of the reaction of 2-methylpyridine-5-carbaldehyde, **11**, and 2-methylpyrimidine-5-carbaldehyde, **1**, with iPr_2Zn are compared. The theoretically calculated rate constants are then introduced in the rate equations of the extended dimer model to spot the role of the second aza group in the 3-position of the aromatic ring. In the third subsection, results of DFT calculations of the reaction of **1** with Me_2Zn, iPr_2Zn, and tBu_2Zn are compared with the aim of explaining the effect of the dialkylzinc structure. Our main findings are summarized in the Conclusions section.

COMPUTATIONAL METHODS

A number of putative energy minimum conformations for each species were generated by rotations around the most significant dihedrals. These structures were preoptimized at the semiempirical PM3D level (proprietary modification of the PM3 method[16] implemented in Spartan 06[17]) and then subjected to further optimization without any symmetry constraint at the M05-2X/6-31G(d) level of theory with the program Gaussian 03.[18] The M05-2X was the functional of choice because it was recently demonstrated to outperform the popular B3LYP functional in the energetic description of organic systems,[19] and was recommended as the most suitable one for accurate calculations of geometries and energetics of Zn compounds.[20] The global energy minimum of each species was then selected as the representative structure. Transition states were located by the quadratic synchronous transit method (QST2)[21] and characterized by frequency calculations. The eigenvector relative to the imaginary frequency of each transition state was carefully inspected to check that it corresponded to the expected reaction coordinate. Electronic energies (hartree) and

Scheme 3. Blackmond−Brown (Homochiral−Homocatalytic) Dimer Model

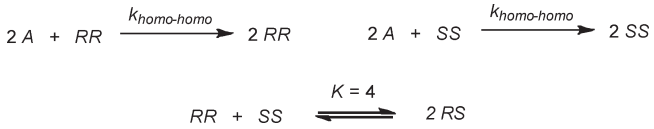

Cartesian coordinates (Å) of M05-2X/6-31G(d) optimized structures are reported in the Supporting Information.

RESULTS AND DISCUSSION

Formal Kinetics of the Extended Dimer Model. In a previous paper we proposed that the catalytic cycle outlined in Scheme 2 and its mirror image constitute the dominant mechanism in the case of the reaction of **1** with iPr_2Zn.[11b] The cycle is characterized by the formation of the hexamolecular complex **6**-*R,anti-R,anti-P*. From the point of view of formal kinetics, should the mechanism be limited to the catalytic cycle outlined in Scheme 2 and its mirror image, the evolution of the ee is described by the BB dimer model, outlined in Scheme 3.[22]

The BB dimer model is constituted by two irreversible reactions representing the two enantiomeric homochiral-homocatalytic cycles and by the fast metathesis equilibrium between homo- and heterodimers that is only dictated by statistics ($K = 4$). Although the mechanistic complexity expressed by the autocatalytic cycle of Scheme 2 and its mirror image may appear in contrast with the simplicity of the BB dimer model, such reduction is absolutely rigorous from the point of view of formal kinetics provided that all the association equilibria are fast and reversible, that iPr_2Zn is strongly associated to the alkoxide dimers and it is in excess with respect to the sum of aldehyde and alkoxyde catalyst, and that the rate-determining step is the conversion of the complex **6** into the complex **7**.[22]

The function describing the ee evolution as a function of reaction turnover and initial ee of the product catalyst has been obtained by analytic integration of the rate equations relative to Scheme 3.[10] According to this function, ee continuously increases to become practically equal to 1 provided a sufficient amount of aldehyde is available.

Although the autocatalytic cycle outlined in Scheme 2 and its mirror image is the dominant mechanism for the specific case of the reaction of **1** with iPr_2Zn, we pointed out that in the general case there are ten chiral hexamolecular complexes of type **6**, each with a distinct mirror image, whose structures depend on the chirality of the monomeric units of the dimer and on the arrangement of the two aldehyde and iPr_2Zn units.[11b] The 20 hexamolecular complexes of type **6** imply that in principle there are 20 distinct catalytic cycles in competition with each other, half of which are mirror images of the other half.[11b] For example, the reaction of **9** with iPr_2Zn, leading to depletion of chirality, cannot be explained by the operation of the cycle of Scheme 2 and its mirror image only, because these two cycles would lead to chiral amplification; in this case the operation of other catalytic cycles must be also considered.

Each of the 20 possible catalytic cycles can be tagged with one of the following five labels: homochiral-homocatalytic (homo-homo), homochiral-enantiocatalytic (homo-enantio), homochiral-heterocatalytic (homo-hetero), heterochiral-homocatalytic (hetero-homo), and heterochiral-heterocatalytic (hetero-hetero),

depending on the chirality of the monomeric units of the dimer catalyst and on the specific arrangement of the given hexamolecular complex that dictates the type of asymmetric catalysis brought about by the dimer in the catalytic cycle. Accordingly, a most general version of the dimer model can be formulated as shown in Scheme 4.

From the point of view of formal kinetics, the extended dimer model shown in Scheme 4 can be somewhat simplified by merging some processes. Indeed considering that, owing to the metathesis equilibrium, the production of one mole of *RS* corresponds to the production of half a mole each of *RR* and *SS*, and vice versa, the homochiral-heterocatalytic cycle producing one mole of *RS* can be merged into both the homochiral-homocatalytic and the homochiral-enantiocatalytic cycles by assuming it contributes to both the cycles with half a mole each. Accordingly, we can define the kinetic constant for the apparent process of homochiral-homocatalysis as eq 1, and that for the apparent process of homochiral-enantiocatalysis as eq 2.

$$k'_{homo\text{-}homo} = k_{homo\text{-}homo} + {}^1/_2 k_{homo\text{-}hetero} \quad (1)$$

$$k'_{homo\text{-}enantio} = k_{homo\text{-}enantio} + {}^1/_2 k_{homo\text{-}hetero} \quad (2)$$

Similarly, the catalytic cycles in which the catalyst is the heterochiral dimer can be grouped into a single formally achiral cycle by defining the kinetic constant for the apparent process of heterochiral-heterocatalysis as eq 3.

$$k'_{hetero\text{-}hetero} = 2k_{hetero\text{-}homo} + 2k_{hetero\text{-}hetero} \quad (3)$$

After these mergings Scheme 4 reduces to Scheme 5.[23]

Note that if the homodimers exclusively reproduce themselves (strict autocatalysis) $k'_{homo\text{-}enantio} = 0\ M^{-2}\ s^{-1}$, and if the heterodimer is inactive as catalyst $k'_{hetero\text{-}hetero} = 0\ M^{-2}\ s^{-1}$. Under these conditions, the extended dimer model (Scheme 5) reduces to the basic dimer model (Scheme 3).

From the rate and equilibrium equations related to Scheme 5, one can obtain the derivative of ee with respect to the total concentration of the monomeric catalyst-product *C* as shown in eq 4:[22]

$$\frac{dee}{dC} = \frac{ee}{C}\left(\frac{2k_1 - 1 - ee^2}{2k_2 + 1 + ee^2}\right) \quad (4)$$

where the constants k_1 and k_2 are defined by eqs 5 and 6.

$$k_1 = \frac{k'_{homo\text{-}homo} - k'_{homo\text{-}enantio} - k'_{hetero\text{-}hetero}}{k'_{homo\text{-}homo} + k'_{homo\text{-}enantio} - k'_{hetero\text{-}hetero}} \quad (5)$$

$$k_2 = \frac{k'_{hetero\text{-}hetero}}{k'_{homo\text{-}homo} + k'_{homo\text{-}enantio} - k'_{hetero\text{-}hetero}} \quad (6)$$

By equating eq 4 to 0, one obtains the stationary value of ee given by eq 7:

$$ee_{st} = \sqrt{2k_1 - 1} \quad (7)$$

It can be shown that the value of ee_{st} is larger than 0 only if the condition in eq 8 is satisfied, corresponding to $k_1 > 0.5$.[22]

$$k'_{homo\text{-}homo} > 3k'_{homo\text{-}enantio} + k'_{hetero\text{-}hetero} \quad (8)$$

If the condition in eq 8 holds, two situations can occur: (i) the initial ee is larger than ee_{st}, in this case the derivative is negative, meaning that ee decreases on increasing the conversion up to reach ee_{st} (limited chiral depletion), and (ii) the initial ee is smaller than ee_{st}, then ee increases up to reach ee_{st} (limited chiral amplification). Note that in the BB dimer model $k_1 = 1$ and $k_2 = 0$, thus $ee_{st} = 1$ (unlimited chiral amplification).

In contrast, if the condition in eq 8 is not satisfied the derivative in eq 4 is always negative, independently of the value of ee, meaning that ee decreases up to racemization (unlimited chiral depletion).

Analytic integration of eq 4 is reported in the Supporting Information.

Of course the ee evolution obtained by analytic integration of the rate laws of classical kinetics can explain chiral amplification but it is unable to reproduce the mirror-image symmetry breaking occurring in the Soai reaction. The spontaneous emergence of chirality from achiral reactants is an important characteristic of the Soai reaction[3] that can possibly manifest itself when discrete numerical simulations of putative mechanisms are carried out.[6g,i] For example, Micheau et al. showed that, due to the automatic adaptation of the integration step size, small fluctuations are introduced into the calculations that can reveal dynamic instabilities inherent to the system. Such fluctuations can trigger the transition from an unstable racemic to a stable optically active

Scheme 4. Extended Dimer Model[a]

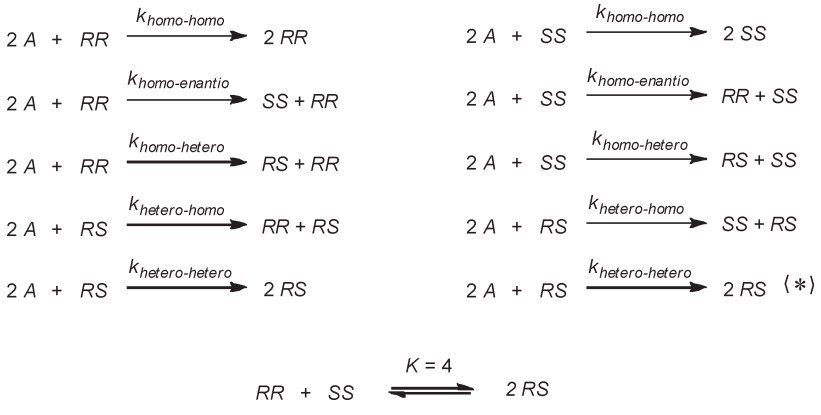

[a] Note that the cycles in which the heterochiral dimer is engaged are also chiral, thus also the mirror images of such cycles have to be considered; the hetero−hetero cycle on the right is marked with an asterisk to distinguish it from its mirror image on the left.

dx.doi.org/10.1021/jo102525t |*J. Org. Chem.* 2011, 76, 2619–2626

Scheme 5. Simplified Extended Dimer Model[a]

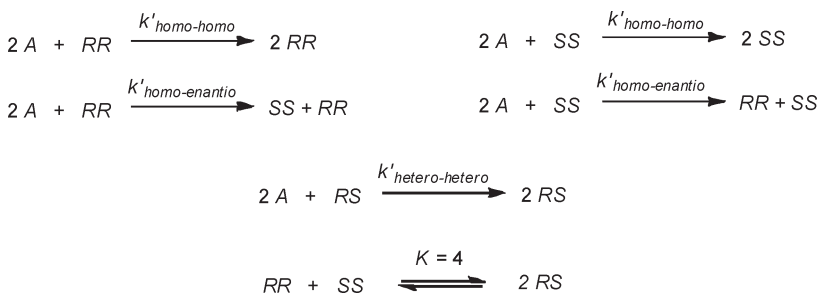

[a] Note that the cycle in which the heterochiral dimer is engaged is no longer considered chiral.

Table 1. M05-2X/6-31G(d) Relative Electronic Energies (Kcal mol^{-1}) of the 10 Chiral Hexamolecular Complexes 6 and of the TSs Separating Each Complex 6 from the Indicated Complex 7[a]

entry	cycle tag	complex **6**	$\Delta E_{\text{complex 6}}$	TS (**6** → **7**)	ΔE_{TS}
1	*homo-homo*	**6**-*R,anti-R,anti-P*	0.0	TS (→ 7-*R,anti-RR*)	6.8
2	*homo-homo*	**6**-*R,anti-R,anti-M*	5.7	TS (→ 7-*R,anti-RR*)	17.1
3	*hetero-homo*	**6**-*R,anti-S,syn-P*	2.9	TS (→7-*R,anti-SR*)	9.0[b]
4	*homo-hetero*	**6**-*R,anti-R,syn-M*	9.8	high energy TS	>13[c]
5	*hetero-homo*	**6**-*R,anti-S,syn-M*	12.6	high energy TS	>16[c]
6	*homo-hetero*	**6**-*R,anti-R,syn-P*	1.4	TS (→ 7-*R,anti-RS*)	8.5[d]
7	*homo-enantio*	**6**-*S,syn-S,syn-P*	6.9	TS (→ 7-*S,syn-SR*)	12.0
8	*hetero-hetero*	**6**-*S,syn-R,syn-M*	14.1	high energy TS	>17[c]
9	*homo-enantio*	**6**-*R,syn-R,syn-P*	3.5	TS (→ 7-*R,syn-RS*)	14.2
10	*hetero-hetero*	**6**-*R,anti-S,anti-P*	7.8	high energy TS	>11[c]

[a] Data refer to the reaction of 2-methylpyrimidine-5-carbaldehyde, **1**, with *i*Pr$_2$Zn. Not corrected for ZPE. [b] The ΔE_{TS} of the TS leading to the formation of 7-*S,syn-RR* is 14.4 kcal mol^{-1}. [c] Estimated limit value (see text). [d] The ΔE_{TS} of the TS leading to the formation of 7-*R,syn-RR* is 9.7 kcal mol^{-1}.

state if (and only if) the system is in a mirror symmetry breaking domain.[6i]

Effect of the Second Aza Group in the Six-Membered Aromatic Ring of the Aldehydic Substrate. To understand the reasons why pyrimidine-5-carbaldehydes are better than pyridine-3-carbaldehydes as substrates for the Soai reaction (amplification vs depletion of chirality), we carried out a comparison between the reactions of substrates **1** and **11** with *i*Pr$_2$Zn, calculated at the M05-2X/6-31G(d) level of theory. Initially we planned to compare the reactions of substrates **9** and **10**, lacking the methyl group in the 2-position, since these two substrates have a direct bearing on the experimental data cited in the Introduction. However, our initial attempts to optimize the geometries of complexes of type **6** for these two substrates were frustrated by the fact that the lack of the methyl group makes these complexes conformationally much more mobile thus making the location of the global minimum more laborious and uncertain. This difficulty convinced us to focus our study on the reactions of substrates **1** and **11**. By the way, the reduced conformational mobility of complexes of type **6** when a substituent is present in the 2-position could explain, in terms of a larger preorganization, why a 2-substituent is beneficial to chiral amplification.

In Table 1 are reported data from our previous work relative to the reaction of substrate **1**.[11b] In particular are reported the relative electronic energies of the 10 chiral hexamolecular complexes of type **6** and those of the rate-determining transition states (TSs) separating the complexes **6** from the corresponding complexes **7**. The nomenclature of the complexes **6** and **7** was explained in our previous work[11b] and does not need to be reiterated here. The energies of some of the TSs in Table 1 were not computed because they were predicted to be significantly higher than that of the lowest energy TS, equal to 6.8 kcal mol^{-1} (entry 1). This prediction is based on the fact that the corresponding complexes **6** have an energy greater than this value by not less than 0.5 kcal mol^{-1} and by the consideration that, on going toward the TS, the energy must necessarily further increase; a conservative estimate of such increase is not less than ca. 3 kcal mol^{-1}, giving the estimated limit values for ΔE_{TS} shown in the table. The unsymmetrical complexes **6** (entries 3 and 6) can give rise to two distinct TSs depending on which side of the complex reacts; in Table 1 is reported the energy of the lower energy of the two TSs, while that of the other one is reported as a note to the table.

Since the resting state of all the catalytic cycles is constituted by isoergonic zinc-saturated dimers, the kinetic constant of each catalytic cycle can be expressed as function of the kinetic constant of the *homo-homo* cycle by eq 9. Electronic energy differences (ΔE_{TS}) are used in eq 9 rather than Gibbs energy differences (ΔG_{TS}) because it is assumed that entropy and thermal contributions to enthalpy for the various transition states are comparable and cancel each other in the difference $\Delta G_{\text{TS}} - \Delta G_{\text{TS}(homo\text{-}homo)}$.

$$k = k_{homo\text{-}homo} \exp\left(-\frac{\Delta E_{\text{TS}} - \Delta E_{\text{TS}(homo\text{-}homo)}}{RT}\right) \qquad (9)$$

Comparing the cycles with the same tag and selecting, among these, the transition state of lower energy, i.e. $\Delta E_{\text{TS}(homo\text{-}homo)}$ = 6.8 kcal mol^{-1}, $\Delta E_{\text{TS}(homo\text{-}enantio)}$ = 12.0 kcal mol^{-1}, $\Delta E_{\text{TS}(homo\text{-}hetero)}$ = 8.5 kcal mol^{-1}, $\Delta E_{\text{TS}(heter\text{-}ohomo)}$ = 9.0 kcal mol^{-1}, and $\Delta E_{\text{TS}(hetero\text{-}hetero)}$ > 11 kcal mol^{-1}, one can calculate by eq 9 the following kinetic constants at 273.15 K (expressed in $k_{homo\text{-}homo}$ units): $k_{homo\text{-}homo}$ = 1.0, $k_{homo\text{-}enantio}$ = 6.9 × 10^{-5}, $k_{homo\text{-}hetero}$ = 4.4 × 10^{-2}, $k_{hetero\text{-}homo}$ = 1.7 × 10^{-2}, $k_{hetero\text{-}hetero}$ < 4.4 × 10^{-4}. With these values the kinetic constants appearing in Scheme 5 (expressed in $k_{homo\text{-}homo}$ units) are calculated by eqs 1−3 as $k'_{homo\text{-}homo}$ = 1.0, $k'_{homo\text{-}enantio}$ = 2.2 × 10^{-2}, and $k'_{hetero\text{-}hetero}$ = 3.6 × 10^{-2}. These values satisfy the condition in eq 8 and allow in turn the evaluation of the constant k_1 (= 0.96) by eq 5, and then ee_{st} (= 0.96) by eq 7. The ee_{st} value is in tremendously good agreement with experimental results regarding the reaction of **1** in toluene at 0 °C,[24] showing that if the initial ee of the catalyst **2**

dx.doi.org/10.1021/jo102525t |*J. Org. Chem.* 2011, 76, 2619–2626

Table 2. M05-2X/6-31G(d) Relative Electronic Energies (kcal mol^{-1}) of the 10 Chiral Hexamolecular Complexes 12 and of the TSs Separating Each Complex 12 from the Indicated Complex 13[a]

entry	cycle tag	complex 12	$\Delta E_{\text{complex 12}}$	TS (12 → 13)	ΔE_{TS}
1	*homo-homo*	**12**-*R,anti-R,anti-P*	0.7	TS (→ **13**-*R,anti-RR*)	7.8
2	*homo-homo*	**12**-*R,anti-R,anti-M*	5.1	TS (→ **13**-*R,anti-RR*)	16.3
3	*hetero-homo*	**12**-*R,anti-S,syn-P*	3.4	TS (→**13**-*R,anti-SR*)	9.6[b]
4	*homo-hetero*	**12**-*R,anti-R,syn-M*	9.3	high energy TS	>12[c]
5	*hetero-homo*	**12**-*R,anti-S,syn-M*	12.2	high energy TS	>15[c]
6	*homo-hetero*	**12**-*R,anti-R,syn-P*	0.0	TS (→ **13**-*R,anti-RS*)	7.8[d]
7	*homo-enantio*	**12**-*S,syn-S,syn-P*	7.4	TS (→ **13**-*S,syn-SR*)	13.6
8	*hetero-hetero*	**12**-*S,syn-R,syn-M*	13.7	high energy TS	>17[c]
9	*homo-enantio*	**12**-*R,syn-R,syn-P*	1.5	TS (→ **13**-*R,syn-RS*)	12.6
10	*hetero-hetero*	**12**-*R,anti-S,anti-P*	7.8	TS (→ **13**-*S,anti-RR*)	11.9[e]

[a] Data refer to the reaction of 2-methylpyridine-5-carbaldehyde, **11**, with iPr$_2$Zn. Not corrected for ZPE. [b] The ΔE_{TS} of the TS leading to the formation of **13**-*S,syn-RR* is 11.3 kcal mol^{-1}. [c] Estimated limit value (see text). [d] The ΔE_{TS} of the TS leading to the formation of **13**-*R,syn-RR* is 9.3 kcal mol^{-1}. [e] The ΔE_{TS} of the TS leading to the formation of **13**-*R,anti-SS* is 15.6 kcal mol^{-1}.

is larger than 0.96, depletion of chirality occurs to reach the experimental ee$_{st}$ value of 0.96, whereas if it is lower than 0.96, amplification of chirality occurs to reach the experimental ee$_{st}$ value of 0.95. Such a high value of ee$_{st}$ is due to the dominant role of the homochiral-homocatalytic cycle shown in Scheme 2 which has a transition state energy significantly lower (entry 1 in Table 1) than those of the other catalytic cycles.

In Table 2 are reported data relative to the reaction of substrate **11** with the same caveats indicated for Table 1. The structures of complexes **12** (not shown) are the same as those of complexes **6** when allowance is made for the change of the substrate structure from **1** to **11**. By the same token, the structures of the rate-determining TSs separating the complexes **12** from the corresponding complexes **13** are analogous to those separating the complexes **6** from the corresponding complexes **7**.

In the case of substrate **11** the ΔE_{TS} of the TSs of lower energy with different cycle tag are as follows: $\Delta E_{TS(homo\text{-}homo)}$ = 7.8 kcal mol^{-1}, $\Delta E_{TS(homo\text{-}enantio)}$ = 12.6 kcal mol^{-1}, $\Delta E_{TS(homo\text{-}hetero)}$ = 7.8 kcal mol^{-1}, $\Delta E_{TS(hetero\text{-}homo)}$ = 9.6 kcal mol^{-1}, and $\Delta E_{TS(hetero\text{-}hetero)}$ = 11.9 kcal mol^{-1}. These data allow the calculation by eq 9 of the following kinetic constants at 273.15 K (expressed in $k_{homo\text{-}homo}$ units): $k_{homo\text{-}homo}$ = 1.0, $k_{homo\text{-}enantio}$ = 1.4 × 10^{-4}, $k_{homo\text{-}hetero}$ = 1.0, $k_{hetero\text{-}homo}$ = 3.6 × 10^{-2}, $k_{hetero\text{-}hetero}$ = 5.2 × 10^{-4}. With these values the kinetic constants appearing in Scheme 5 (expressed in $k_{homo\text{-}homo}$ units) are calculated by eqs 1−3 as $k'_{homo\text{-}homo}$ = 1.5, $k'_{homo\text{-}enantio}$ = 0.5, and $k'_{hetero\text{-}hetero}$ = 7.4 × 10^{-2}. These values do not satisfy the condition in eq 8, and thus it is predicted that the initial ee will decrease to racemization (unlimited chiral depletion) provided a sufficient amount of substrate **11** is available. The difference in the behavior of substrates **11** and **1** is striking and is in line with the experimentally observed behaviors of substrates **10** and **9**. The presence of a second aza group in the six-membered aromatic ring leads to amplification of chirality, whereas its absence leads to depletion of chirality. This different behavior is ascribed to the fact that the absence of the second aza group makes the homochiral-heterocatalytic cycle (entry 6 in Table 2) competitive with the homochiral-homocatalytic cycle (entry 1 in Table 2), causing an increase of the constant $k'_{homo\text{-}enantio}$. Although the effect of the additional aza group can be calculated and shown to agree with experimental data, it cannot be easily explained on the basis of traditional steric and electronic effects used by physical organic chemists to rationalize the course of organic reactions.

Effect of Dialkylzinc Structure. To understand why iPr$_2$Zn plays a crucial role for the effectiveness of the Soai reaction, we carried out a comparison between the reactions of substrate **1** with Me$_2$Zn, iPr$_2$Zn, and tBu$_2$Zn, calculated at the M05-2X/6-31G(d) level of theory. Dimethyl- and di-*tert*-butylzinc were selected because they are sterically less and more encumbered, respectively, than diisopropylzinc, and because the rotational symmetry of the corresponding alkyl groups reduces the number of possible conformations thus simplifying the calculations. Data for the reaction of iPr$_2$Zn are collected in Table 1. In Table 3 are reported data relative to the reaction substrate **1** with Me$_2$Zn with the same caveats indicated for Table 1. The structures of complexes **14** (not shown) are the same as those of complexes **6** when allowance is made for the change of the dialkylzinc structure from iPr$_2$Zn to Me$_2$Zn. By the same token, the structures of the rate-determining TSs separating the complexes **14** from the corresponding complexes **15** are analogous to those separating the complexes **6** from the corresponding complexes **7**.

In the case of Me$_2$Zn reacting with substrate **1** the ΔE_{TS} of the TSs of lower energy with different cycle tag are the following: $\Delta E_{TS(homo\text{-}homo)}$ = 8.9 kcal mol^{-1}, $\Delta E_{TS(homo\text{-}enantio)}$ = 12.5 kcal mol^{-1}, $\Delta E_{TS(homo\text{-}hetero)}$ = 10.0 kcal mol^{-1}, $\Delta E_{TS(hetero\text{-}homo)}$ = 9.2 kcal mol^{-1}, and $\Delta E_{TS(hetero\text{-}hetero)}$ = 9.1 kcal mol^{-1}. These data allow the calculation by eq 9 of the following kinetic constants at 273.15 K (expressed in $k_{homo\text{-}homo}$ units): $k_{homo\text{-}homo}$ = 1.0, $k_{homo\text{-}enantio}$ = 1.3 × 10^{-3}, $k_{homo\text{-}hetero}$ = 1.3 × 10^{-1}, $k_{hetero\text{-}homo}$ = 5.8 × 10^{-1}, $k_{hetero\text{-}hetero}$ = 6.9 × 10^{-1}. With these values the kinetic constants appearing in Scheme 5 (expressed in $k_{homo\text{-}homo}$ units) are calculated by eqs 1−3 as $k'_{homo\text{-}homo}$ = 1.1, $k'_{homo\text{-}enantio}$ = 6.7 × 10^{-2}, and $k'_{hetero\text{-}hetero}$ = 2.5. These values do not satisfy the condition in eq 8, and thus it is predicted that the initial ee will decrease to racemization (unlimited chiral depletion) provided a sufficient amount of substrate **1** is available. The comparison between the reactions of iPr$_2$Zn and Me$_2$Zn shows that with the latter both the heterochiral-homocatalytic (entry 5 in Table 3) and the heterochiral-heterocatalytic (entry 10 in Table 3) cycles are competitive with the homochiral-homocatalytic cycle (entry 2 in Table 3), causing an increase of the constant $k'_{hetero\text{-}hetero}$. The effect is due to the lower steric hindrance of Me$_2$Zn that makes the energies of all the TSs more similar to each other.

As to the reaction of substrate **1** with tBu$_2$Zn, we first focused our attention to the hexamolecular complex **16**-*R,anti-R,anti-P*, analogous to the complex **6**-*R,anti-R,anti-P*, the only difference

dx.doi.org/10.1021/jo102525t |J. Org. Chem. 2011, 76, 2619–2626

Table 3. M05-2X/6-31G(d) Relative Electronic Energies (kcal mol^{-1}) of the 10 Chiral Hexamolecular Complexes 14 and of the TSs Separating Each Complex 14 from the Indicated Complex 15[a]

entry	cycle tag	complex 14	$\Delta E_{\text{complex 14}}$	TS (14 → 15)	ΔE_{TS}
1	*homo-homo*	**14**-*R,anti-R,anti-P*	6.4	TS (→ **15**-*R,anti-RR*)	10.5
2	*homo-homo*	**14**-*R,anti-R,anti-M*	0.0	TS (→ **15**-*R,anti-RR*)	8.9
3	*hetero-homo*	**14**-*R,anti-S,syn-P*	6.9	TS (→ **15**-*R,anti-SR*)	10.7[b]
4	*homo-hetero*	**14**-*R,anti-R,syn-M*	9.6	high energy TS	>13[c]
5	*hetero-homo*	**14**-*R,anti-S,syn-M*	3.4	TS (→ **15**-*R,anti-RS*)	9.2[d]
6	*homo-hetero*	**14**-*R,anti-R,syn-P*	2.7	TS (→ **15**-*R,anti-RS*)	10.0[e]
7	*homo-enantio*	**14**-*S,syn-S,syn-P*	7.2	TS (→ **15**-*S,syn-SR*)	12.5
8	*hetero-hetero*	**14**-*S,syn-R,syn-M*	6.0	TS (→ **15**-*S,syn-SR*)	12.8[f]
9	*homo-enantio*	**14**-*R,syn-R,syn-P*	5.9	TS (→ **15**-*R,syn-RS*)	12.5
10	*hetero-hetero*	**14**-*R,anti-S,anti-P*	1.3	TS (→ **15**-*R,anti-SS*)	9.1[g]

[a] Data refer to the reaction 2-methylpyrimidine-5-carbaldehyde, **1**, with Me_2Zn. Not corrected for ZPE. [b] The ΔE_{TS} of the TS leading to the formation of **15**-*S,syn-RR* is 13.4 kcal mol^{-1}. [c] Estimated limit value (see text). [d] The ΔE_{TS} of the TS leading to the formation of **15**-*S,syn-RR* is 12.4 kcal mol^{-1}. [e] The ΔE_{TS} of the TS leading to the formation of **15**-*R,syn-RR* is 11.2 kcal mol^{-1}. [f] The ΔE_{TS} of the TS leading to the formation of **15**-*R,syn-RS* is 13.8 kcal mol^{-1}. [g] The ΔE_{TS} of the TS leading to the formation of **15**-*S,anti-RR* is 10.3 kcal mol^{-1}.

being the change of the dialkylzinc moieties from iPr$_2$Zn to tBu$_2$Zn. The energy change associated to the formation of **16**-*R,anti-R,anti-P* starting from two molecules of aldehyde **1** and one molecule of the corresponding zinc saturated dimer analogous to **4**-R_2, in the gas phase, is just −1.3 kcal mol^{-1} (to be compared with the value of −44.5 kcal mol^{-1} computed in the case of the reaction with iPr$_2$Zn). Such a small value suggests that entropic effects and solvation should make this complex highly unstable in solution and consequently the mechanism in Scheme 2 is precluded when tBu$_2$Zn is used as the organozinc reagent. The latter conclusion gains further support by the failure of all attempts at optimizing a TS structure for tBu transfer from Zn to the closest aldehydic group within the hexamolecular complex. Both these findings are ascribable to the very large steric hindrance of the tBu group, and are more than sufficient to exclude the mechanism in Scheme 2 as a viable route for the reaction with tBu$_2$Zn. In view of the huge computational efforts needed to study such large systems, we did not consider the remaining hexamolecular complexes of type **16** any further.

CONCLUSIONS

There is no shortage of mechanistic proposals for the Soai reaction,[7−11] which are the matter of passionate discussions and hot debate within the scientific community.[25] To date, the dimer model in its basic version (the BB model) is one of the most prominent mechanisms, supported by experimental evidence (kinetics and NMR).[7] Previous DFT calculations disclosed the possibility that the BB model is a particular case of a more general model,[11b] dubbed here as the extended dimer model. It includes 20 distinct catalytic cycles in competition with each other, half of which are mirror images of the other half. According to the extended dimer model, the observation of asymmetric amplification in the Soai reaction depends on the dominance of the homochiral homocatalytic cycles over the other catalytic cycles leading to dissipation of chirality. It is shown here that this dominance is due to a fine-tuning of the structure of the aldehydic substrate and of the dialkylzinc reagent. As to the substrate, the results show that a small structural change such as the introduction of a second aza group in the aromatic ring implies a modest energetic advantage of the homochiral-homocatalytic cycles over the homochiral-heterocatalytic ones, but this small advantage is more than enough to dramatically change the behavior of the reaction from chiral depletion to chiral amplification. The steric hindrance of the dialkylzinc reagent is also critical; the results show that both a reduction and an increase of the steric hindrance with respect to iPr$_2$Zn cause chiral depletion. Indeed, in the case of Me_2Zn chiral depletion is due to a leveling out of the rates of the competing catalytic cycles, whereas in the case of tBu$_2$Zn, chiral depletion is due to the instability of the hexamolecular complexes possibly making other unselective addition mechanisms more viable. In conclusion, the data reported here clearly indicate that the chiral amplification observed in the Soai reaction is due to a specific combination of structural and kinetic factors. The agreement between our theoretical results and some puzzling literature experiments is a strong argument to confirm that in the Soai reaction, homochiral and heterochiral dimers, and possibly higher aggregates, are taking part in various competitive catalytic cycles.

ASSOCIATED CONTENT

Supporting Information. Reduction of the Autocatalytic Cycle of Scheme 2 to the BB Model; analytic integration of the simplified extended dimer model; full author listing for ref 18; and electronic energies and Cartesian coordinates. This material is available free of charge via the Internet at http://pubs.acs.org.

AUTHOR INFORMATION

Corresponding Author

*E-mail: ercolani@uniroma2.it; luca.schiaffino@uniroma2.it.

REFERENCES

(1) (a) Soai, K.; Shibata, T.; Morioka, H.; Choji, K. *Nature* **1995**, *378*, 767–768. (b) Soai, K.; Shibata, T.; Sato, I. *Acc. Chem. Res.* **2000**, *33*, 382–390. (c) Soai, K.; Kawasaki, T. *Chirality* **2006**, *18*, 469–478. (d) Soai, K.; Kawasaki, T. *Top. Curr. Chem.* **2008**, *284*, 1–33. (e) Gehring, T.; Busch, M.; Schlageter, M.; Weingand, D. *Chirality* **2010**, *22*, E173–E182.

(2) Singleton, D. A.; Vo, L. K. *J. Am. Chem. Soc.* **2002**, *124*, 10010–10011.

(3) (a) Patent: Soai, K.; Shibata, T.; Kowata, Y. Japan Kokai Tokkyo Koho JP, 9-268179, 1997. (b) Soai, K.; Sato, I.; Shibata, T.; Komiya, S.; Hayashi, M.; Matsueda, Y.; Imamura, H.; Hayase, T.; Morioka, H.; Tabira, H.; Yamamoto, J.; Kowata, Y. *Tetrahedron: Asymmetry* **2003**,

14, 185–188. (c) Gridnev, I. D.; Serafimov, J. M.; Quiney, H.; Brown, J. M. *Org. Biomol. Chem.* **2003**, *1*, 3811–3819. (d) Singleton, D. A.; Vo, L. K. *Org. Lett.* **2003**, *5*, 4337–4339. (e) Kawasaki, T.; Suzuki, K.; Shimizu, M.; Ishikawa, K.; Soai, K. *Chirality* **2006**, *18*, 479–482. (f) Barabas, B.; Caglioti, L.; Zucchi, C.; Maioli, M.; Gál, E.; Micskei, K.; Pályi, G. *J. Phys. Chem. B* **2007**, *111*, 11506–11510. (g) Micskei, K.; Rábai, G.; Gál, E.; Caglioti, L.; Pályi, G. *J. Phys. Chem. B* **2008**, *112*, 9196–9200. (h) Suzuki, K; Hatase, K.; Nishiyama, D.; Kawasaki, T.; Soai, K. *J. Syst. Chem.* **2010**, *1*, 5.

(4) Soai, K.; Osanai, S.; Kadowaki, K.; Yonekubo, S.; Shibata, T.; Sato, I. *J. Am. Chem. Soc.* **1999**, *121*, 11235–11236.

(5) (a) Kawasaki, T.; Matsumura, Y.; Tsutsumi, T.; Suzuki, K.; Ito, M.; Soai, K. *Science* **2009**, *324*, 492–495. (b) Kawasaki, T.; Shimizu, M.; Nishiyama, D.; Ito, M.; Ozawa, H.; Soai, K. *Chem. Commun.* **2009**, 4396–4398.

(6) (a) Sato, I.; Omiya, D.; Tsukiyama, K.; Ogi, Y.; Soai, K. *Tetrahedron: Asymmetry* **2001**, *12*, 1965–1969. (b) Sato, I.; Omiya, D.; Igarashi, H.; Kato, K.; Ogi, Y.; Tsukiyama, K.; Soai, K. *Tetrahedron: Asymmetry* **2003**, *14*, 975–979. (c) Buhse, T. *Tetrahedron: Asymmetry* **2003**, *14*, 1055–1061. (d) Rivera Islas, J.; Lavabre, D.; Grevy, J.-M.; Hernandez Lamoneda, R.; Rojas Cabrera, H.; Micheau, J.-C.; Buhse, T. *Proc. Natl. Acad. Sci. U.S.A.* **2005**, *102*, 13743–13748. (e) Saito, Y.; Hyuga, H. *J. Phys. Soc. Jpn.* **2004**, *73*, 33–35. (f) Saito, Y.; Hyuga, H. *J. Phys. Soc. Jpn.* **2004**, *73*, 1685–1688. (g) Crusats, J.; Hochberg, D.; Moyano, A.; Ribó, J. M. *ChemPhysChem* **2009**, *10*, 2123–2131. (h) Busch, M.; Schlageter, M.; Weingand, D.; Gehring, T. *Chem.—Eur. J.* **2009**, *15*, 8251–8258. (i) Micheau, J.-C.; Cruz, J.-M.; Coudret, C.; Buhse, T. *ChemPhysChem* **2010**, *11*, 3417–3419.

(7) (a) Blackmond, D. G.; McMillan, C. R.; Ramdeehul, S.; Schorm, A.; Brown, J. M. *J. Am. Chem. Soc.* **2001**, *123*, 10103–10104; (b) Buono, F. G.; Blackmond, D. G. *J. Am. Chem. Soc.* **2003**, *125*, 8978–8979; (c) Gridnev, I. D.; Serafimov, J. M.; Brown, J. M. *Angew. Chem.* **2004**, *116*, 4992–4995; *Angew. Chem., Int. Ed.* **2004**, *43*, 4884–4887. (d) Gridnev, I. D.; Brown, J. M. *Proc. Natl. Acad. Sci. U.S.A.* **2004**, *101*, 5727–5731. (e) Gridnev, I. D. *Chem. Lett.* **2006**, *35*, 148–153. (f) Brown, J. M.; Gridnev, I. D.; Klankermayer, J. *Top. Curr. Chem.* **2008**, *284*, 35–65.

(8) Although at present the dimer model seems to be the mechanism with the largest body of experimental evidence (ref 7), there are hints suggesting that in the case of 2-alkynylpyrimidine-5-carbaldehydes, tetramers and/or higher oligomers might play a dominant role (refs 9 and 10).

(9) (a) Klankermayer, J.; Gridnev, I. D.; Brown, J. M. *Chem. Commun.* **2007**, 3151–3153. (b) Quaranta, M.; Gehring, T.; Odell, B.; Brown, J. M.; Blackmond, D. G. *J. Am. Chem. Soc.* **2010**, *132*, 15104–15107.

(10) Schiaffino, L.; Ercolani, G. *ChemPhysChem* **2009**, *10*, 2508–2515. Corrigendum: *ChemPhysChem* **2010**, *11*, 2060.

(11) (a) Schiaffino, L.; Ercolani, G. *Angew. Chem.* **2008**, *120*, 6938–6941; *Angew. Chem., Int. Ed.* **2008**, *47*, 6832–6835. (b) Schiaffino, L.; Ercolani, G. *Chem.—Eur. J.* **2010**, *16*, 3147–3156.

(12) Lowry, T. H.; Richardson, K. S. In *Mechanism and Theory in Organic Chemistry*, 3rd ed.; Harper & Row: New York, 1987; p 190.

(13) For an analysis of the influence of the aldehyde structure, see: Lavabre, D.; Micheau, J.-C.; Islas, J. R.; Buhse, T. *Top. Curr. Chem.* **2008**, *284*, 67–96 and references cited therein.

(14) Soai, K.; Niwa, S.; Hori, H. *J. Chem. Soc., Chem. Commun.* **1990**, 982–983.

(15) Soai, K.; Niwa, S. *Chem. Rev.* **1992**, *92*, 833–856.

(16) Stewart, J. J. P. *J. Mol. Model* **2004**, *10*, 155–164 and references cited therein.

(17) *Spartan 06*; Wavefunction, Inc., Irvine, CA.

(18) *Gaussian 03*, Revision-E.01; Frisch, M. J. et al. ; Gaussian, Inc., Pittsburgh, PA, 2009.

(19) Wodrich, M. D.; Corminboeuf, C.; Schreiner, P. R.; Fokin, A. A.; Schleyer, P. v. R. *Org. Lett.* **2007**, *9*, 1851–1854.

(20) (a) Amin, E. A.; Truhlar, D. G. *J. Chem. Theory Comput.* **2008**, *4*, 75–85. (b) Sorkin, A.; Truhlar, D. G.; Amin, E. A. *J. Chem. Theory Comput.* **2009**, *5*, 1254–1265.

(21) Peng, C.; Schlegel, H. B. *Isr. J. Chem.* **1993**, *33*, 449–454.

(22) See the Supporting Information for details.

(23) A kinetic scheme in which $k'_{hetero\text{-}hetero} = 0$ was analytically integrated in a previous work (ref 10). In that work $k'_{homo\text{-}homo}$ was indicated as k_{ret}, and $k'_{homo\text{-}enantio}$ as k_{inv}, where the subscripts *ret* and *inv* stood for chiral retention and chiral inversion, respectively.

(24) Shibata, T.; Morioka, H.; Hayase, T.; Choji, K.; Soai, K. *J. Am. Chem. Soc.* **1996**, *118*, 471–472.

(25) *2nd International Symposium on the Soai Reaction and Related Topics*; Felsőmocsolád (Somogy County, Hungary); September 11—13, 2010.